NCEP NOTES

An Operational System for Predicting Hurricane-Generated Wind Waves in the North Atlantic Ocean*

YUNG Y. CHAO, JOSE-HENRIQUE G. M. ALVES,+ AND HENDRIK L. TOLMAN+

Marine Modeling and Analysis Branch, NOAA/NCEP/Environmental Modeling Center, Camp Springs, Maryland

(Manuscript received 5 March 2004, in final form 10 September 2004)

ABSTRACT

A new wind–wave prediction model, referred to as the North Atlantic hurricane (NAH) wave model, has been developed at the National Centers for Environmental Prediction (NCEP) to produce forecasts of hurricane-generated waves during the Atlantic hurricane season. A detailed description of this model and a comparison of its performance against the operational western North Atlantic (WNA) wave model during Hurricanes Isidore and Lili, in 2002, are presented. The NAH and WNA models are identical in their physics and numerics. The NAH model uses a wind field obtained by blending data from NCEP's operational Global Forecast System (GFS) with those from a higher-resolution hurricane prediction model, whereas the WNA wave model uses winds provided exclusively by the GFS. Relative biases of the order of 10% in the prediction of maximum wave heights up to 48 h in advance, indicate that the use of higher-resolution winds in the NAH model provides a successful framework for predicting extreme sea states generated by a hurricane. Consequently, the NAH model has been made operational at NCEP for use during the Atlantic hurricane season.

1. Introduction

There is a critical need to improve the skill of operational forecasts of extreme wind–wave fields associated with intense hurricanes, because of the potentially damaging impacts they can have on coastal settlements and economic activities. Hence, the National Centers for Environmental Prediction (NCEP) have implemented two specialized wave models to provide regional forecasts of hurricane-generated wind waves in the North Atlantic and Pacific Ocean basins on an operational basis: the North Atlantic and North Pacific hurricane wave models, NAH and NPH.

The NAH and NPH models are part of the National Oceanic and Atmospheric Administration's (NOAA) WAVEWATCH III (NWW3) wave forecasting system, which also includes a global model, and three other regional models covering the following domains: Alaskan waters (AKW), western North Atlantic (WNA), and eastern North Pacific (ENP). All models in the NWW3 suite are implementations of the third-generation spectral ocean wave model WAVEWATCH III (Tolman et al. 2002). A detailed description of the regional NWW3 wave forecasting system and of some of its applications may be found in Chao et al. (1999a,b) and Chao et al. (2001, 2002). All wave models in the NWW3 system are driven with wind forecasts from NCEP's Global Forecast System (GFS; Moorthi et al. 2001), previously known as Medium-Range Forecast (MRF) and Aviation (AVN) models (Caplan et al. 1997). Hurricane-generated wave models are driven with GFS winds blended with higher-resolution winds, as will be described below.

It is well known that the details of intense and rapidly varying wind fields associated with tropical cyclones are poorly resolved by large-scale global circulation models such as the GFS. The main reasons for this are that the

* Marine Modeling and Analysis Branch Contribution Number 246.

+ Additional affiliation: Science Applications International Corporation/GSO, Beltsville, Maryland.

Corresponding author address: Jose-Henrique Alves, NOAA/NCEP/Environmental Modeling Center, Rm. 209, 5200 Auth Rd., Camp Springs, MD 20746.
E-mail: Henrique.Alves@NOAA.gov

intrinsic spatial and temporal resolutions of global models are usually too coarse to resolve the wind field structure associated with a relatively small hurricane vortex (Surgi et al. 1998; Chao et al. 2001). For the GFS model, the spatial resolution is of the order of 50 km in latitude–longitude, while wind fields are available only at 3-h intervals. As a result, predicted wave heights in areas under the influence of tropical storms are usually unrealistically low and do not accurately reflect the temporal changes in the properties of storm wave fields (see below and Chao and Tolman 2001; Chao and Tolman 2001, unpublished manuscript).

To provide more accurate forecasts of storm tracks and wind intensities, NCEP uses a specialized hurricane prediction model during hurricane seasons to provide additional forecast guidance for NOAA's National Hurricane Center (NHC). This model, developed at the Geophysical Fluid Dynamics Laboratory (GFDL), is a multiply nested, movable mesh model involving variable grid resolutions (for details, see Kurihara et al. 1998). At NCEP, the GFDL model is implemented with two nested movable grids consisting of a finer inner mesh centered at the hurricane and an outer coarse mesh (see below). This implies that the GFDL model can only target one storm at a time. When multiple storms exist simultaneously, a single targeted storm is centered in the inner grid, while other storms appear in the coarse outer mesh. Therefore, the details of wind fields associated with storms in the outer mesh again may not be adequately described.

Since only one storm can be tracked per GFDL model run, the combined effects of various wind fields from coexisting storms on generating wind waves cannot be adequately predicted using the output of a single GFDL model run. However, when multiple storms coexist, independent GFDL model runs are made at NCEP targeting each storm individually. From the perspective of wave modeling, this introduces two problems. First, no single forecast product is available with optimal high-resolution wind fields for all hurricanes. This is a key issue for simulating hurricane wave fields from multiple storms because swell systems generated by individual storms propagate far away from the generating storm. Second, the GFDL grids often do not cover the entire wave model domain, which is fixed.

The solution to these problems is to blend higher-resolution GFDL winds within the area of influence of each hurricane with GFS winds outside the storm area, thus providing a single wind field covering the entire wave model domain. Both the NAH and NPH wave models incorporate such a procedure for an arbitrary number of hurricanes (Chao and Tolman 2000, 2001). The NAH model, the main focus of the present study, has been operational at NCEP since June 2001. Its domain extends from the equator to 50°N and from 98° to 30°W. This domain is identical to that of the WNA regional wave model, which has been operational at NCEP since March 2000. The fundamental difference between the WNA and NAH models is that the former is driven exclusively with GFS winds, while the latter is forced with blended GFDL and GFS winds, as mentioned above.

In this paper we review the development of the NAH wave model and investigate in more detail its performance during the 2002 hurricane season. Our performance assessment of NAH is made relative to wave forecasts generated by the WNA model. In section 2 we describe the procedure for blending GFS and GFDL model winds. In section 3, we describe the methodology used to forecast hurricane waves using blended wind fields. Section 4 summarizes previous results obtained during the development and testing stages of the NAH wave model. The validation of predicted winds and waves against buoy measurements is presented in sections 5 and 6. We provide a discussion focusing on the results, limitations, and outlook for future improvements to the NCEP hurricane wave forecasting models in section 7. Finally, our concluding remarks are presented in section 8.

2. Wind field specification for hurricane wave models

The GFS atmospheric model currently operational at NCEP (Moorthi et al. 2001) provides basic wind information for the WNA and NAH models, as well as for all other wave models under the NWW3 model suite. The GFS model runs four cycles per day for 0000, 0600, 1200, and 1800 UTC. It generates global forecasts at 3-h intervals out to 180 h, and at lower spatial and temporal resolution out to 16 days. The presently operational GFDL hurricane model also runs four cycles per day at 0000, 0600, 1200, and 1800 UTC. Regular outputs of the GFDL model are made available to the general public at 6-h intervals out to 126 h. A separate dataset consisting of hourly sea level pressure and wind fields at GFDL model's lowest layer (about 35 m from the surface), out to 72 h, is specially generated for use in wave forecasts.

Since the initial period of development and testing of the NAH model (see below), the GFDL model has undergone substantial modifications. The first version of the GFDL model used to drive the NAH wave model had three spatial grids with horizontal resolutions ranging from 1° to 1/3° to 1/6° covering an area of 75° × 75°, 11° × 11°, and 5° × 5° in latitude–longitude,

respectively (Kurihara et al. 1998). Modifications incorporated since then and up to the year 2002 hurricane season included improvements in hurricane initialization (Liu et al. 2000), the implementation of a hurricane–ocean coupling kernel (Bender et al. 2001), and the implementation of the current two-nested-grid configuration (Bender et al. 2002).

Since the 2002 hurricane season and up to the present, data from NCEP's GFDL model have been provided at two grid resolutions. The coarse grid has uniform 1/3° resolution covering an area of 75° × 75° in latitude–longitude. The inner, finer nested mesh has a uniform 1/6° grid resolution covering an area of 11° × 11° in latitude–longitude. At any given time step, the center of the finer mesh is aligned to a single storm center and, therefore, moves with the storm as it propagates. The outer, coarse grid has fixed north and south boundaries at 65°N and 10°S, but moves freely on the west–east axis following the storm center.

Since an individual GFDL hurricane model run can only target a single storm, several runs are needed when more than one storm exists. Thus, discrepancies in the wind field features for the same storm but from different GFDL model runs may occur. Furthermore, the storm center and extent of wind field forecast by GFDL and GFS may also have discrepancies. To obtain a single representative description of each system, the concept of area of influence (AOI) for each storm is introduced.

Various definitions of AOIs have been considered and tested, resulting in the following procedure being used to determine the wind field structure for hurricane wave prediction within the NWW3 wave prediction system:

(a) construct the underlying 10-m height wind fields on a regular latitude–longitude grid at 0.5° resolution from the lowest σ-level outputs generated by the GFS model, assuming neutral atmospheric stratification;
(b) interpolate 10-m height GFS winds from 3-h intervals to hourly intervals and to the NAH grid at a 0.25° resolution;
(c) interpolate the hourly GFDL mean sea level pressure field and the lowest-layer wind on coarse and fine grids to the wave model grid resolution and adjust winds to 10-m height, assuming neutral atmospheric stratification;
(d) locate the hurricane eye (lowest sea level pressure) based on the GFDL model mean sea level pressure field;
(e) from the storm center, determine a box area extending outward to the north, south, east, and west until its sides intersect the 1015-mb isobar, using the GFDL model surface pressure field;
(f) determine a second box area extending from the hurricane eye to where the wind speed decreases to 7.5 m s^{-1} or less on each side of the box, based on the GFDL wind field;
(g) similarly, based on the GFS wind field, determine a third box area extending from the hurricane center to where the wind speed decreases to 7.5 m s^{-1} or less on each side of the box;
(h) form a new box area with sides defined as the largest distance to the hurricane eye among the sides of the three boxes defined in steps e–g; and
(i) restrict the box sides to be at angular distances less than or equal to 12.5° and greater than or equal to 3.5° from the hurricane eye in case the box defined in step h violates this criterion.

The area so specified is assumed to be the AOI of any given storm. GFS winds within each AOI are replaced with GFDL winds. To warrant a smooth transition from GFDL winds inside each AOI to GFS winds in the outer storm domains, a weighted-average procedure using linear coefficients is employed within bands with a fixed width of five model grid points (i.e., 1.25°) surrounding the AOI. A similar procedure is employed when two or more AOIs overlap. For more details about the procedure outlined above, see Chao and Tolman (2001).

3. Procedure for predicting hurricane waves

The Atlantic hurricane season formally runs from 1 June to 1 December. On the NWW3 Web site (http://polar.ncep.noaa.gov/waves/), NAH model results are displayed only within this time window unless a tropical storm is identified (e.g., Hurricanes Odette and Peter, between 4 and 11 December 2003). For practical reasons, however, the NAH model is run all year-round by NCEP Central Operations (NCO). The NAH model is kept running even when no GFDL winds are available, to ensure proper tracking of swell systems generated by preexisting hurricanes even when the system has long ceased to exist. In such conditions, the WNA and NAH models share identical surface winds fields, provided by the GFS model.

When output fields from GFDL model runs (i.e., mean sea level pressure and surface winds) are available, the procedure for wind field specification previously described is initiated. The resulting blended surface wind fields are used to force the NAH wave model, while boundary wave conditions at the edges of the NAH model domain are defined as in all other regional

wave models at NCEP, that is, from two-dimensional wave spectra produced by the global wave model.

Like all other models that comprise the NWW3 wave model suite, the NAH model runs four times per day at 0000, 0600, 1200, and 1800 UTC. However, unlike most other models, NAH (and NPH) forecasts extend only out to 72 h, because this is the current time window for availability of hourly data from GFDL model runs. (This limit has been extended to 126 h starting at the 2004 hurricane season.) In all domains covered by the NWW3 system, each model cycle run includes a 6-h wave hindcast that precedes the actual forecasts. Wave hindcasts in models driven exclusively with GFS winds (global, AKW, WNA, and ENP) are generated using 3-hourly analyses from GFS's Global Data Assimilation System (GDAS) for a 6-h period preceding the current cycle's UTC time stamp. Unlike the GFS, the GFDL model does not include a system that assimilates observations for generating analysis fields prior to each model cycle. Therefore, the NAH wave model hindcasts are generated using the GFS analysis winds blended with GFDL winds for the 0–4-h range from the previous cycle (-6 to -2 h range in the current cycle). Wind data at the -1 h time of the current cycle are obtained by interpolating the -2 h winds with the blended GFS–GFDL 0-h wind nowcast. This guarantees a smooth transition between short-term forecasts and the ensuing analysis.

4. Model development and testing

The first version of the NAH wave model was implemented for the 2000 Atlantic hurricane season. This earlier model implementation proved the concept that more accurate hurricane wave forecasts required a specialized model implementation using higher-resolution winds. In this section we provide a brief summary of major findings and improvements made during the first two years of operation of the NAH model. A more detailed evaluation of this development and testing phase is provided in Chao and Tolman (2000) and Chao and Tolman (2001, unpublished manuscript). These papers, which were the basis for the development of the current hurricane wave model implementations at NCEP, report the performance of the NAH model using four case studies: Hurricanes Floyd and Gert (1999 season) and Gordon and Helene (2000 season).

Results from Chao and Tolman (2000) and Chao and Tolman (2001, unpublished manuscript) indicate that for intense hurricanes poorly resolved by the GFS model, more realistic GFDL winds typically resulted in more intense wave conditions. However, some cases were found in which the GFS model correctly predicted the intensity of relatively weak and small systems, but overestimated its spatial extend. Consequently, the WNA model overestimated wave conditions, whereas the NAH correctly predicted lower wave heights. Hence, it was found that for hurricane wave predictions it was not sufficient to simply increase the intensity of underresolved systems. Instead, a generally better depiction of these small-scale features in the high-resolution GFDL model proved to be critical, justifying the approach of blended wind fields, instead of, for instance, using statistically enhanced wind fields such as the bias correction procedure described in Tolman (1998).

The first two years of NAH model operation also revealed some shortcomings of the initial model configuration. For practical reasons, we initially had access to GFDL wind fields at 6-h intervals only. This resulted in problems with the interpolation in time of wind fields for fast-moving systems. This problem became particularly obvious for Hurricane Michelle in 2001, as shown by Chao and Tolman (2001). To mitigate this problem, access to NCEP's GFDL model hourly surface wind field outputs was provided specifically for the wave model. Positive impacts of these changes to hurricane wave forecasting are also described in Chao and Tolman (2001).

Another important change implemented during the development and testing phase of the NAH model was a modification to the AOI scheme, to ensure that the GFS representation of each hurricane is properly replaced (covered) by the AOI. A detailed description of this procedure is provided in section 3 above. This more mature version of the NAH model was implemented for the 2002 hurricane season and is the focus of the present study. This version was also the basis for the NPH model implementation in 2003.

5. Selected events from the 2002 hurricane season

During the hurricane season of 2002, most storms were either far from the east coast of the United States or were not strong enough to generate severe wave conditions near the National Data Buoy Center (NDBC) buoy network in the North Atlantic Ocean. Two hurricanes, however, had a devastating impact in the Gulf of Mexico, occurring within less than a week of each other over the period between 18 September and 7 October. Due to their strength and the extreme wave conditions observed in that period, these hurricanes, named Isidore and Lili, will be the focus of our validation study.

Our validation strategy is based on a comparative assessment of the WNA and NAH model perfor-

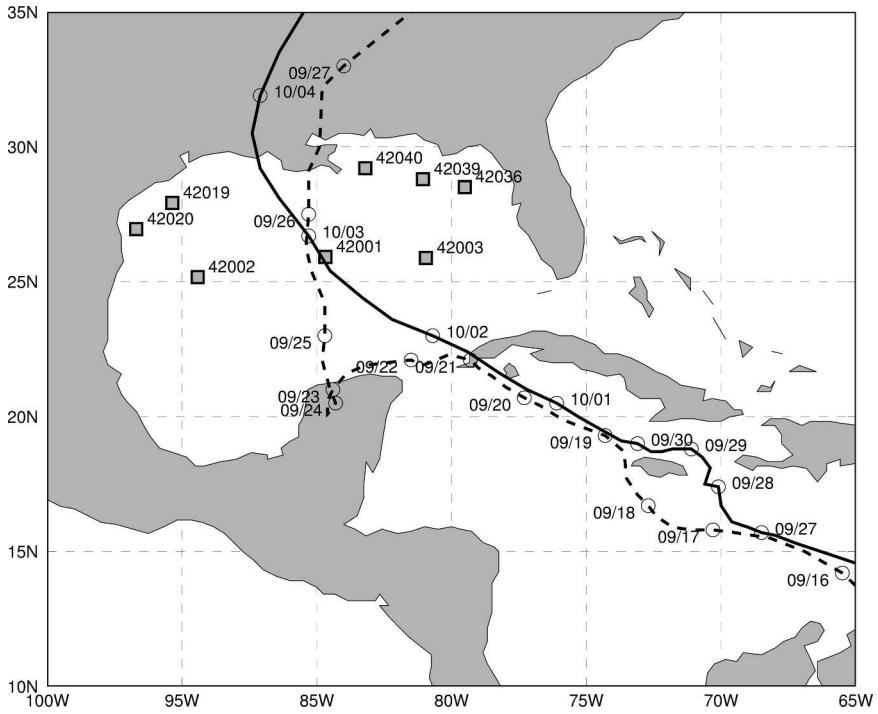

FIG. 1. Location of selected NOAA/NDBC buoys and best-track data for Hurricanes Isidore (dashed line) and Lili (solid line). Daily 0000 UTC positions are also indicated.

mances, using NDBC buoy observations as a reference. Model performance is evaluated in terms of hindcasts and forecasts of the 10-m wind speed (U_{10}), the significant wave height (H_s), and the peak wave period (T_p). Validation is performed against wave parameters recorded at eight NOAA/NDBC buoys deployed in intermediate and deep waters within the Gulf of Mexico. Figure 1 shows tracks of Hurricanes Isidore and Lili, along with the locations of the eight NDBC buoys used in this study. The main characteristics of the NDBC buoys are given in Table 1.

Figures 2–4 show time series of U_{10}, H_s, and T_p, respectively, obtained from NDBC buoys and model hindcasts from WNA and NAH. Model data were generated via interpolation of outputs from surrounding grid points to the buoy location. The listing hierarchy used in these figures, from top to bottom, show deeper to shallower water buoy locations as given in Table 1. The first three buoys (42001, 42002, and 42003) are deployed in the deep Gulf region, whereas the remaining buoys are distributed along the western (42019 and 42020) and eastern (42036, 42039, and 42040) coastal regions of the Gulf.

a. General characteristics of Hurricane Isidore

Hurricane Isidore evolved from a succession of westward-moving tropical depressions near Jamaica, becoming a hurricane on 19 September 2002, at 0800 UTC. On 21 September the storm entered the Gulf of Mexico, after sweeping the northwestern edge of Cuba and veering westward toward the Yucatan Peninsula, with winds over 110 kt (57 m s^{-1}). After its first landfall, Isidore meandered over land and reentered the Gulf of Mexico moving northward as a tropical storm, until making landfall west of Grand Isle, Louisiana, on 26 September at 0600 UTC.

Figure 2 shows that none of the NDBC buoys were directly in the hurricane path during the first passage of Isidore over the Gulf waters between Cuba and Mexico. On the other hand, wind fields associated with

TABLE 1. NDBC buoys: World Meteorological Organization (WMO) code, location, geographical position, and water column depth (in m).

WMO code	Location	Position		Depth (m)
		Lat (°N)	Lon (°W)	
42001	Mid–Gulf of Mexico	25.92	89.68	3246
42002	West Gulf of Mexico	25.17	94.42	3200
42003	East Gulf of Mexico	25.88	85.95	3164
42039	Pensacola, FL	28.80	86.06	283.5
42040	Mobile South, AL	29.21	88.20	237.7
42019	Freeport, TX	27.92	95.36	82.3
42020	Corpus Christi, TX	26.95	96.70	78.6
42036	West Tampa, FL	28.51	84.51	53.0

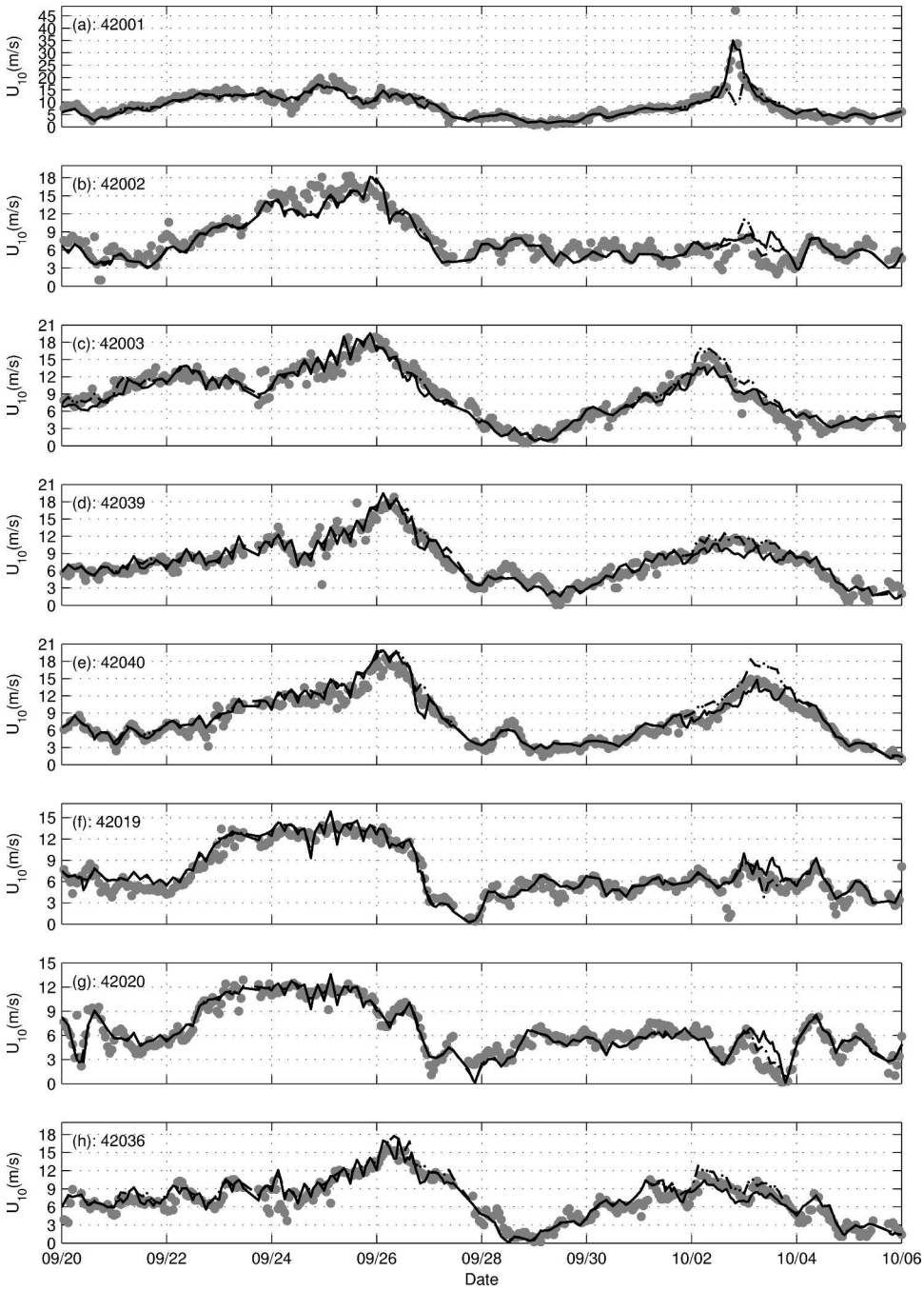

FIG. 2. Time series of U_{10} (m s^{-1}) at selected NOAA/NDBC buoy locations. Hindcast data from the WNA (dashed line) and NAH (solid line) models are compared to observations (gray circles).

Isidore during its second stage directly affected most buoys. Buoys located to the east of the storm track during its second stage (42001, 42003, 42036, 42039, and 42040) were all near the maximum wind region at some time and typically recorded one distinctive U_{10} peak around 25 September (buoy 42001), extending up to 27 September (buoy 42040). Time series of U_{10} recorded at buoys to the west of Isidore's path (42002, 42019, and 42020) were characterized by a "plateau" near $U_{10} = 12$ m s^{-1} during the storm's second stage between 23 and 27 September, as seen in Fig. 2. This plateau reflects the widening of Isidore's western wind sector as it transitioned from a hurricane to a tropical storm.

Isidore's convoluted trajectory generated a complex

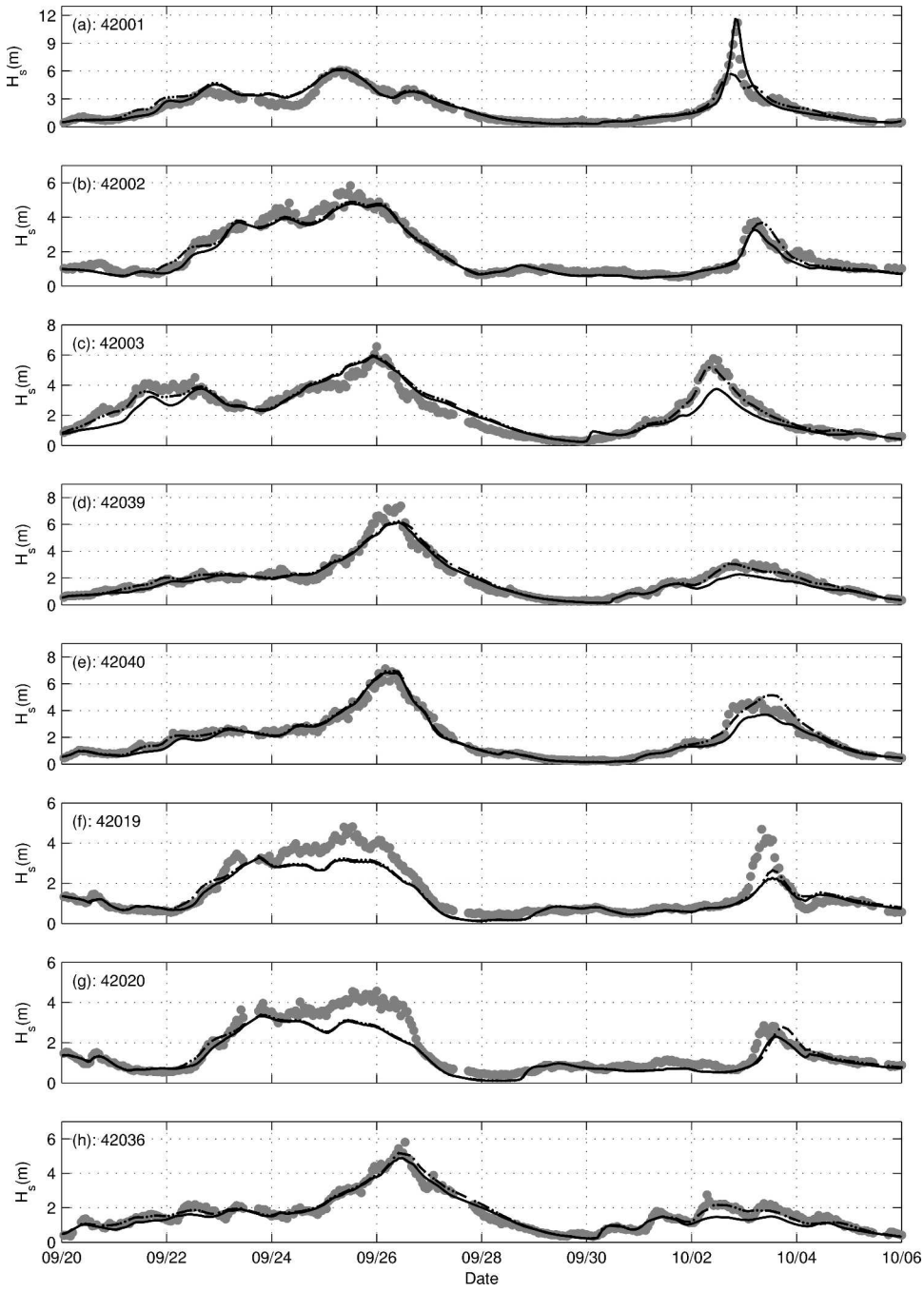

FIG. 3. Time series of H_s (m) at selected NOAA/NDBC buoy locations. Lines and markers are as in Fig. 2.

wave field pattern within the Gulf of Mexico. Even before the hurricane's eye entered the Gulf, swell forerunners were generated by a massive band of storm winds developing in the storm's northern section, near Cuba. After making landfall in the Yucatan Peninsula, Isidore reentered the Gulf and generated local wind seas that superimposed onto these preexisting swells. The resulting wave field patterns were further superimposed by local waves generated by intense southward winds near the coast associated with Isidore's western sector. This complex superposition of wave fields is illustrated in Figs. 3 and 4.

During Isidore's first stage (i.e., 21–23 September), only buoy 42003 recorded a clearly distinguishable sig-

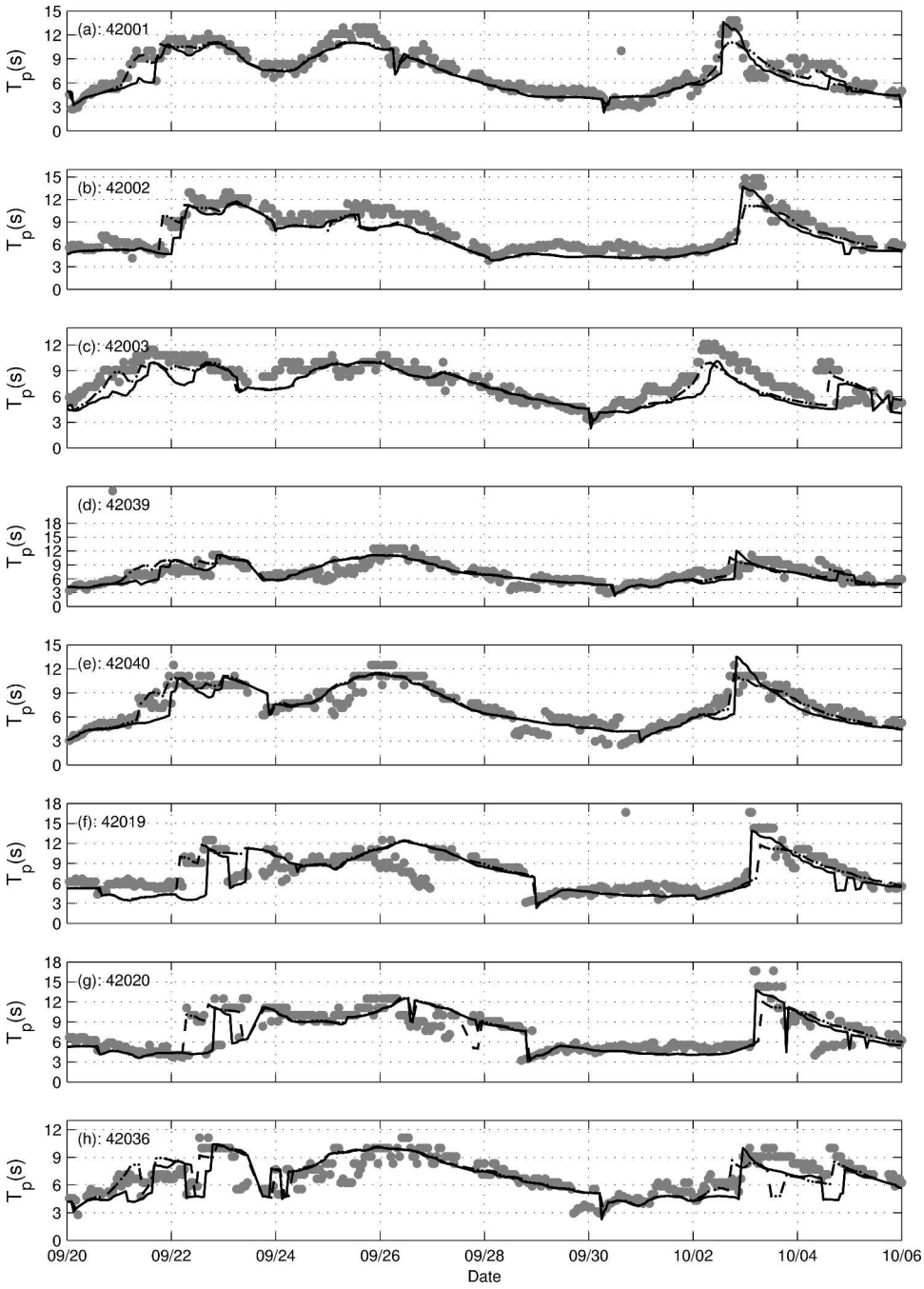

FIG. 4. Time series of T_p (s) at selected NOAA/NDBC buoy locations. Lines and markers are as in Fig. 2.

nal possibly associated with local wind seas generated at the hurricane's maximum wind region. The arrival of swell generated by the hurricane, however, appears as a clear signal in the recorded series of T_p in Fig. 4 as intermittent jumps from around 6 to 12 s between 22 and 24 September.

Buoys 42002, 42019, and 42020 recorded a more complex superposition and sequence of wave field patterns. The first waves to arrive at these locations were swell systems generated during the westward movement of Hurricane Isidore between Cuba and the Yucatan. Their arrival caused a sudden increase in the values of T_p between 23 and 26 September, as shown in Figs. 4b, 4f, and 4g. This was followed by a gradual increase in H_s

(see Fig. 3). Due to the large distance between these buoys and the swell sources, their gradual arrival was mixed with the occurrence of local wind seas.

b. General characteristics of Hurricane Lili

Hurricane Lili started as a depression in the tropical Atlantic Ocean and became a hurricane on 30 September. In the morning of 1 October the storm passed over western Cuba and entered the Gulf of Mexico, with wind speeds as high as 90 kt. The hurricane moved with an advection speed of around 15 kt in a nearly straight northwesterly path. Lili made landfall on the Louisiana coast on 3 October with an estimated 80-kt maximum wind speed, leaving behind 13 deaths and damages of over $860 million. Detailed analyses of Isidore and Lili are provided in Avila (2002) and Lawrence (2002), respectively.

Lili's rather straightforward trajectory generated maximum H_s fields that closely followed the maximum wind path. Lili also generated swell forerunners with noticeable energy propagating westward and northward, radiating from the hurricane track. Soon swell forerunners became the dominant waves in a large area within the Gulf. As the hurricane continued moving northwestward, the fan of swell forerunners widened its area of coverage, sweeping an area spanning from the western coast of Florida to the western reaches of the Campeche Bank in Mexico.

In contrast to Hurricane Isidore, the passage of Hurricane Lili generated a clear rise in wind intensities recorded at buoys located to the east of its track (42001, 42003, 42039, and 42040), while time series of U_{10} from buoys to the west showed little indication of the hurricane's presence (42002, 42019, and 42020), as shown in Fig. 2. Waves generated during the passage of Hurricane Lili over Gulf waters are seen as well-marked peaks in the recorded time series of H_s and T_p at all buoy locations. Wave systems generated before Lili entered the Gulf propagated as swell forerunners and generated peaks in values of T_p at all buoys between 2 and 3 October. Wind seas generated within Lili's northwestward-moving fetch produced a maximum H_s of 11.2 m recorded at buoy 42001 on the evening of 2 October. This was the highest H_s value for the entire period among all buoy locations. Lili's moving fetch also generated swell systems that were recorded as peaks in the time series of H_s at buoys 42002, 42019, and 42020 on 3 October.

6. Validation of model predictions

The evaluation of model performance is made relative to NDBC buoy data. We start with a more general analysis of model performance in terms of standard validation statistics: bias (Bias), root-mean-square error (rmse), rms-error scatter index (SI), and correlation (r). For a definition of these parameters, see Cardone et al. (1996). We then focus on investigating the model performance in terms of predicting the storm peak, represented through maximum or extreme wave heights, at each buoy location.

In all cases the assessment is made of both wave hindcasts and forecasts out to a 72-h forecast horizon. In this way, our performance assessment provides a comprehensive overview of WNA and NAH model performance during the passage of Hurricanes Isidore and Lili through the Gulf of Mexico between 26 September and 6 October 2002.

a. Wind analyses and wave hindcasts

Analyzed wind fields are usually the best available description of the state of the atmosphere during a given period of time in the recent past. Consequently, wave hindcast data based on these wind input fields provide a good opportunity for assessing the skill of the wave model itself and of the quality of the nowcasts issued by the wave forecasting system.

The WNA model hindcast is driven exclusively by analysis winds computed with the aid of measured data assimilated into NCEP's GFS/GDAS, whereas the NAH wave model hindcast uses GFS/GDAS analyses blended with GFDL *forecasts* from a previous model cycle (i.e., no analysis winds are available from GFDL runs). Although this may seemingly lead to lower quality winds being available for the NAH model, the higher-resolution winds available from the GFDL short-range forecast (0–6 h) may compensate for deficiencies in the lower-resolution GFS/GDAS analyses. This seems to be particularly true when hurricanes are present, as suggested by comparisons between pure GFS (WNA) and blended GFS/GFDL (NAH) winds with analysis wind fields provided by NOAA's Hurricane Research Division (HRD; see below). In any case, our performance assessment of wave hindcasts assumes that both WNA and NAH use the best available winds.

Table 1 represents bulk validation statistics of wind intensity U_{10} and wave field parameters H_s and T_p from the WNA and NAH wave models. The differences between the performance of the NAH and WNA models are relatively modest, with WNA slightly outperforming NAH at most buoys located away from the track of both Hurricanes Isidore and Lili. This behavior was most pronounced at buoy 42003, and appears to be related to the cumulative underestimation of Lili's northeast quadrant winds by the GFDL model, which led the NAH model to generate swells that were

TABLE 2. Bulk validation statistics for the combined occurrence period of Hurricanes Isidore and Lili. WNA and NAH wave model results are compared to observations at eight NDBC buoy locations.

		U_{10}				H_s				T_p			
Location	Model	Bias ($m\ s^{-1}$)	Rmse ($m\ s^{-1}$)	SI	r	Bias (m)	Rmse (m)	SI	r	Bias (s)	Rmse (s)	SI	r
42001	WNA	−0.29	2.95	0.36	0.82	0.17	0.60	0.32	0.94	−0.29	1.09	0.15	0.93
	NAH	−0.16	1.61	0.20	0.95	0.13	0.46	0.24	0.97	−0.50	1.28	0.17	0.90
42002	WNA	−0.35	1.50	0.19	0.91	−0.08	0.27	0.15	0.98	−0.83	1.22	0.12	0.94
	NAH	−0.38	1.65	0.21	0.89	−0.17	0.30	0.14	0.98	−1.01	1.25	0.10	0.96
42003	WNA	0.33	1.29	0.15	0.96	0.08	0.37	0.18	0.97	−0.76	1.34	0.15	0.86
	NAH	−0.07	1.28	0.16	0.95	−0.13	0.56	0.27	0.93	−1.05	1.69	0.18	0.80
42039	WNA	0.42	1.25	0.18	0.96	0.02	0.30	0.18	0.98	−0.14	1.67	0.24	0.72
	NAH	0.09	1.26	0.19	0.95	−0.12	0.35	0.20	0.98	−0.36	1.70	0.24	0.72
42040	WNA	0.83	1.40	0.16	0.98	0.06	0.30	0.17	0.99	−0.21	1.05	0.15	0.91
	NAH	0.40	1.21	0.17	0.97	−0.11	0.33	0.18	0.98	−0.44	1.29	0.17	0.88
42019	WNA	0.50	1.09	0.14	0.95	−0.16	0.49	0.32	0.94	−0.19	1.94	0.27	0.74
	NAH	0.49	1.15	0.15	0.94	−0.21	0.51	0.32	0.95	−0.53	2.01	0.27	0.74
42020	WNA	−0.03	0.98	0.15	0.94	−0.24	0.49	0.28	0.93	−0.29	1.99	0.27	0.73
	NAH	−0.03	1.12	0.17	0.92	−0.29	0.49	0.26	0.95	−0.53	1.83	0.24	0.79
42036	WNA	0.69	1.48	0.21	0.94	0.01	0.23	0.16	0.98	−0.06	1.44	0.22	0.74
	NAH	0.30	1.39	0.22	0.92	−0.12	0.29	0.19	0.97	−0.33	1.55	0.23	0.72

weaker than observed at buoy 42003. This problem has been solved in a more recent version of the GFDL model (see below). At buoy 42001, which was the only buoy directly under Lili's track and, thus, exposed to extreme wind intensities, the validation statistics indicate a clear superiority of winds and waves predicted by the NAH model.

The passage of Lili over buoy 42001 occurred when the hurricane was near its maximum intensity. As shown in Fig. 2a, GFDL winds used by the NAH model reproduced more closely Lili's maximum U_{10} profile at buoy 42001 than did the GFS winds in the WNA model. Still, the GFDL model underestimates the observed maximum wind speed by approximately 20%. Such a discrepancy may result from actual mesoscale variabilities in the wind field not reproduced by the GFDL model, or by inaccuracies in the location of maximum winds in a small storm such as Lili. These problems tend to be minimized in a wave model because a wave model responds more strongly to the larger time and space scales in the wind fields and, thus, tends to act as a low-pass filter. On the other hand, underestimated extreme model winds may also have been compensated for in the wave model due to a wind stress parameterization that does not yet include the observed effects of surface drag reduction at very high speeds (Powell et al. 2003; Moon et al. 2004).

Despite these discrepancies and uncertainties, the enhanced performance of the GFDL model winds relative to the GFS model during the passage of Lili over buoy 42001 reflected positively in the validation statistics for H_s: NAH hindcasts of H_s were significantly better than those of the WNA model as seen in Fig. 3a. Though not clearly reflected in statistics for T_p, this improved performance is evident in the time series for T_p near the storm peak, as seen in Fig. 4. These results reveal that the NAH model provides good estimates of extreme wave conditions, which are critical in operational forecasting of hurricane waves.

A conspicuous feature in Table 2 is the comparatively poor performance of both models in terms of hindcast H_s at buoys 42019 and 42020. Through visual inspection of Fig. 3, it is clear that these biases result from an underprediction of H_s between 24 and 27 September (second stage of Isidore's passage over the Gulf of Mexico). Not by chance, the highest bias in computed T_p from both WNA and NAH models occurs for data from buoy 42002 and is closely connected with the model H_s bias in buoys 42019 and 42020 between 26 and 27 September (see Fig. 4). The reason behind these more noticeable discrepancies stems largely from biases in the forcing analyzed surface wind fields used in the wave models.

Although these biases are not clearly seen in the time series of U_{10} shown in Fig. 2, significant sources of biases in the spatial distribution of model wind intensities are revealed when a comparison is made against manual analyses of surface winds made at the Hurricane Research Division of NOAA's Atlantic Oceanographic and Meteorological Laboratory (AOML; Powell et al. 1998). An example of such bias is presented in Fig. 5a, which compares HRD-analyzed winds with surface winds used by the WNA and NAH models at 0130 UTC 22 September. Normally, the hurricane's maxi-

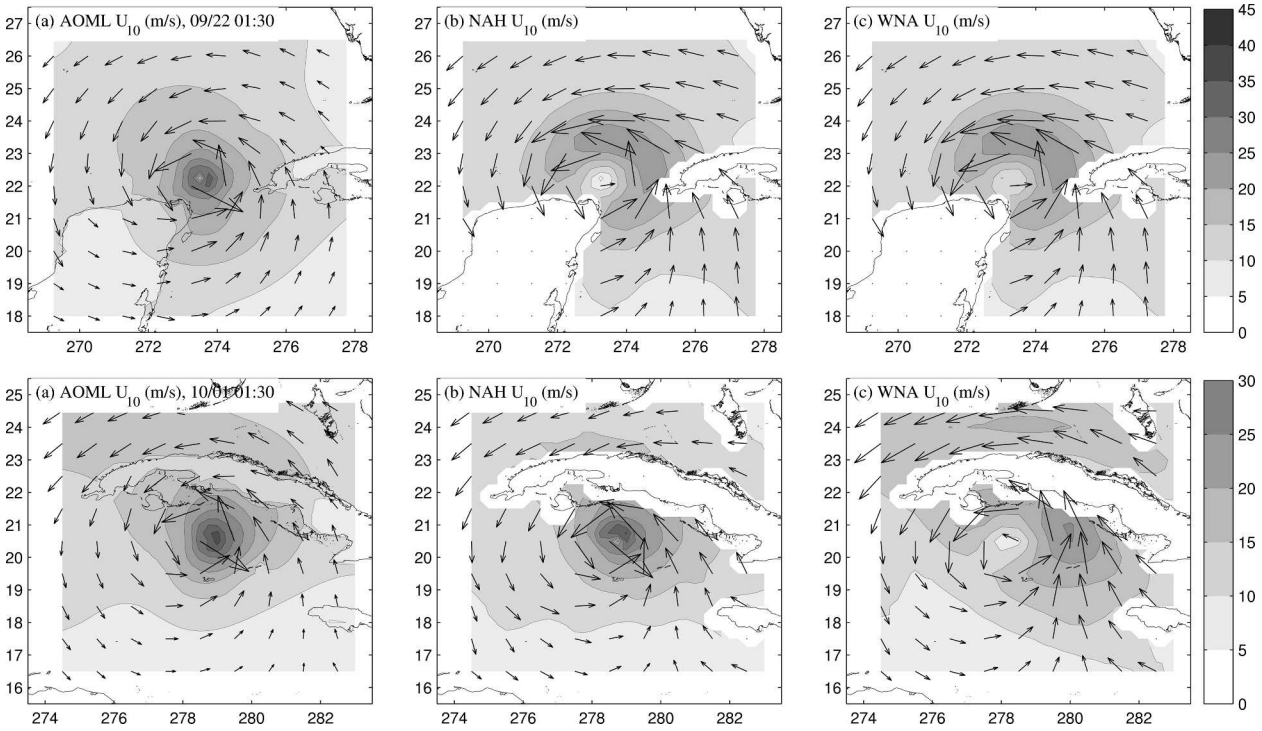

FIG. 5. Comparison of (a) AOML, (b) NAH, and (c) WNA surface winds ($m\ s^{-1}$): (top) Isidore's first crossing of the Gulf of Mexico on 22 Sep and (bottom) and Lili entering the Gulf on 1 Oct.

mum wind region is the strongest source of energy for generating swells. In this special situation, however, the presence of Cuba isolated the maximum wind region from Lili's outer flow. The HRD analyses in Fig. 5a indicate that model winds in Lili's outer flow were much weaker than the actual winds. Consequently, simulated swell fields are significantly weaker than measurements made at buoys 42019 and 42020, as shown in Figs. 3f and 3g.

As mentioned above, the WNA model outperformed the NAH model at buoys 42003, 42039, and 42036—all to the east of Hurricane Lili's path. In these cases, the relatively poorer performance of the NAH model is associated with the generation of weaker swell systems as a consequence of weaker GFDL model winds away from the hurricane's eye (outer wind field sectors) when Lili was entering the Gulf of Mexico, north of Cuba. Figure 5b shows the HRD-analyzed surface winds and the wind fields used by WNA and NAH at 0130 UTC 1 October, the most likely date in which these swell systems were generated. Figure 5b reveals that the stronger wind sector north of Cuba observed in the HRD fields is well approximated by GFS/WNA, but significantly underestimated by the GFDL/NAH winds. This problem resulted from deficiencies in the planetary boundary layer (PBL) closure scheme used in the GFDL model until the end of the 2002 hurricane season. To eliminate this deficiency, the PBL scheme used in the GFS model was implemented onto the GFDL model (T. Marchock 2004, personal communication). The sensitivity of wave model predictions to these changes is discussed in Tolman et al. (2005, in this issue).

b. Wind and wave forecasts

Due to the availability of hourly GFDL winds only out to the 72-h forecast range, our analysis of forecast performance of the NAH and WNA models will also be limited to this forecast period, even though the latter provides products out to 168 h. A convenient way of summarizing the skill of wind and wave model forecasts associated with the NAH and WNA models is illustrated in Figs. 6–9. These figures show the time series of envelopes bounded by maximum and minimum values of U_{10}, H_s, and T_p obtained from all available forecast data ranging from 0 to 72 h. These figures illustrate the range of variability of forecasts at selected buoy sites during the passage of Isidore and Lili through the Gulf of Mexico.

A striking feature of Figs. 6–9 is the relatively modest envelope width, indicating a moderate range of change or variability that implies a high consistency between

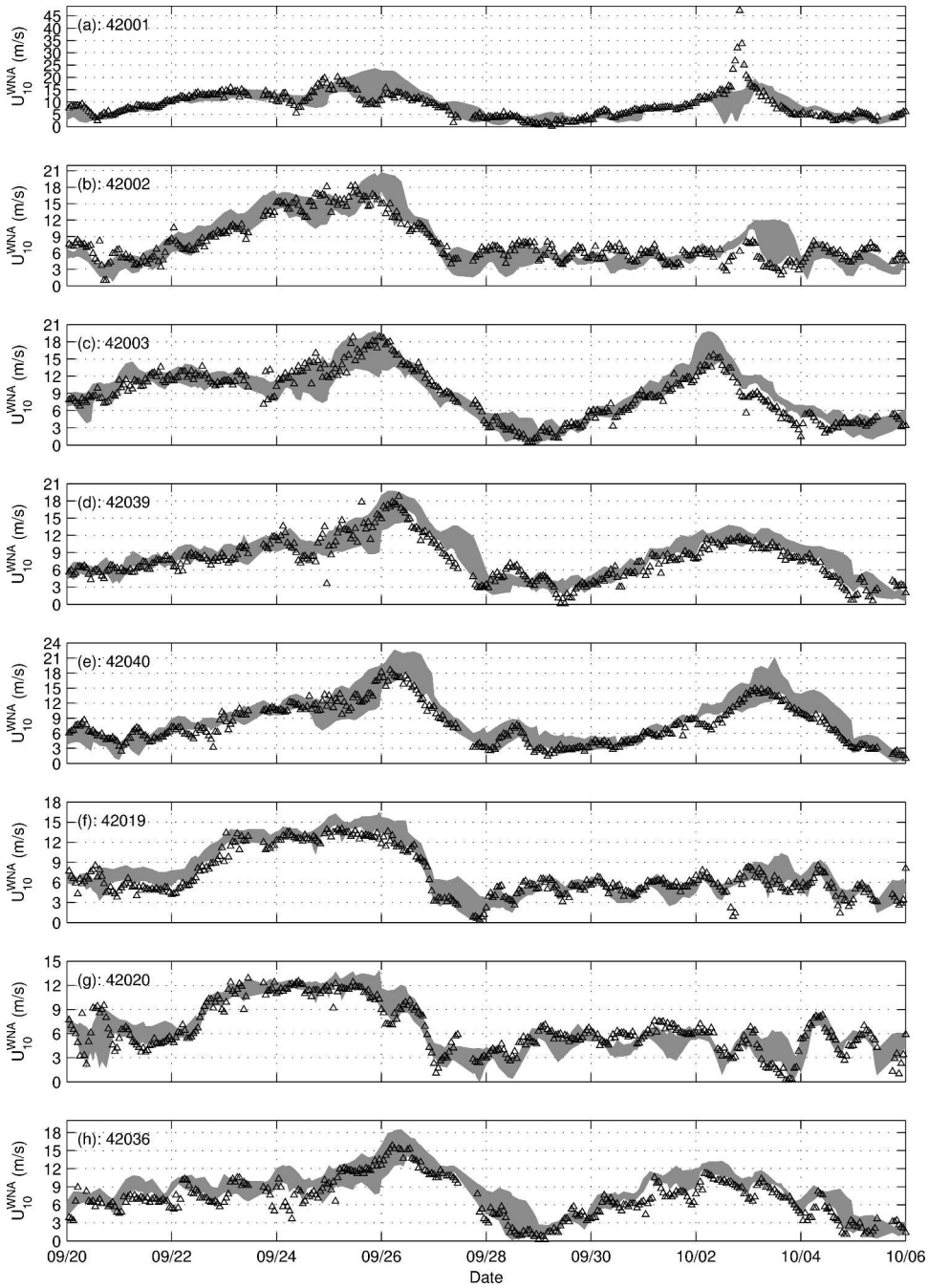

FIG. 6. Time series of the forecast envelope of U_{10} (m s^{-1}) from the WNA (GFS) model. The envelope is built from maxima and minima of all U_{10} data within forecast ranges from 0 to 72 h.

hindcasts and forecasts out to the 72-h forecast horizon. There are, however, several short sections in the diagram showing considerably large envelope widths. A careful examination indicates that these events occurred near the times of arrival of wind seas or swells generated by either Lili or Isidore, suggesting a large change in predicted parameters associated with these hurricanes from one forecast cycle to another. The most obvious reason for that is the expected uncertainty in atmospheric model forecasts of wind intensity within stronger storm systems, particularly in extreme and complex wind conditions associated with hurricanes.

Less obvious, but not least important, is the effect of

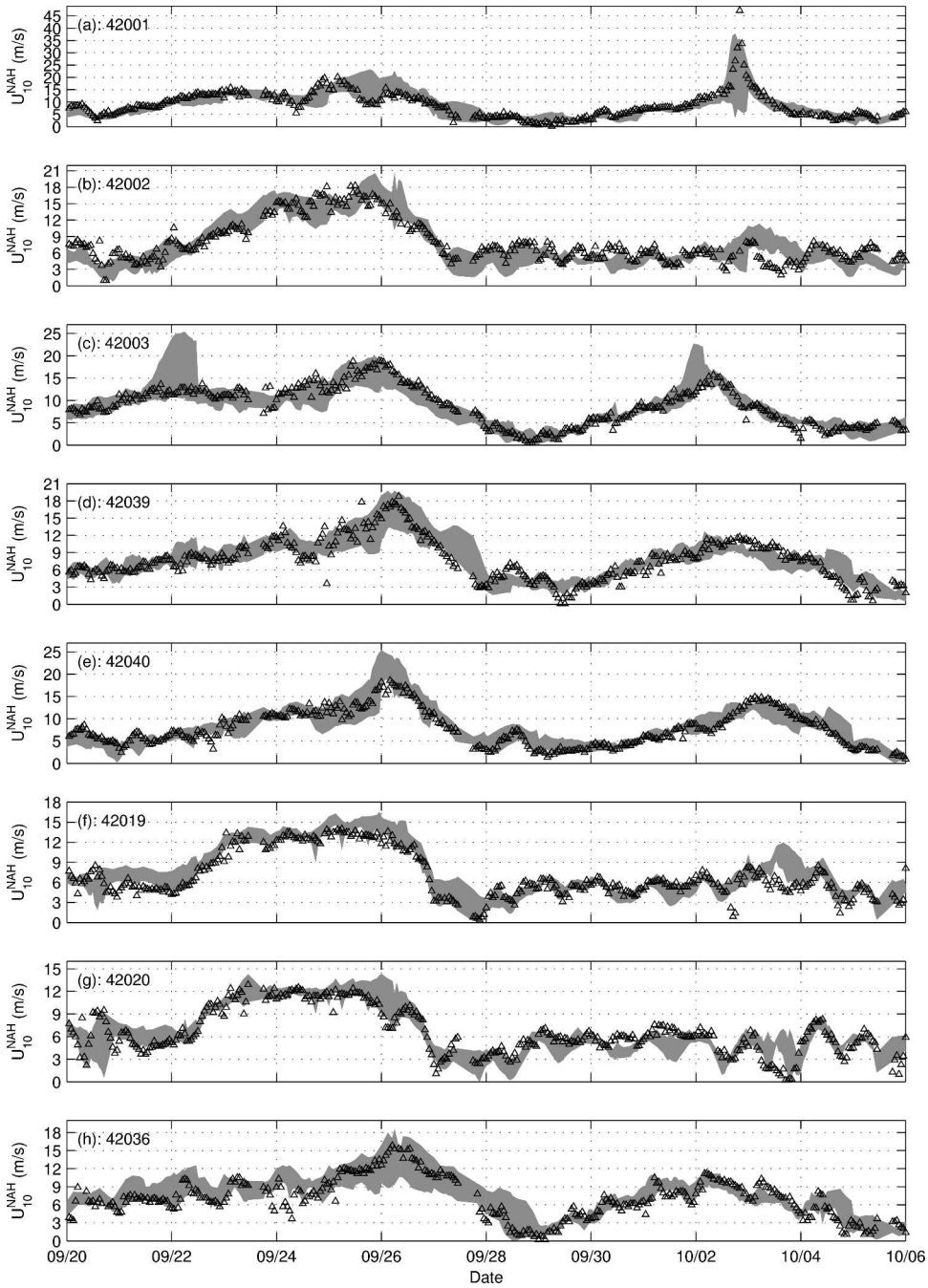

FIG. 7. Forecast envelope for U_{10} (m s^{-1}) from the NAH (GFDL) model, as in Fig. 6.

uncertainties associated with forecasts of the path followed by the two hurricanes. An illustration of the uncertainty in model track forecasts of Hurricanes Isidore and Lili relative to the track data issued by the NCEP's National Hurricane Center (NHC) is shown in Fig. 10. Envelopes of forecast tracks from the GFDL hurricane model, shown in Fig. 10a, reveal that the variability in the predicted position of both hurricanes was quite large within a forecast range of 72 h. In its widest points, the envelope indicates an uncertainty of up to 5° of latitude, which is on the order of magnitude of the size of the hurricane systems themselves. As is to be expected, uncertainties grow and the forecast track envelope widens as the forecast range grows, being relatively small and very close to the NHC best-track analysis for a forecast range of 0–24 h. Forecast track enve-

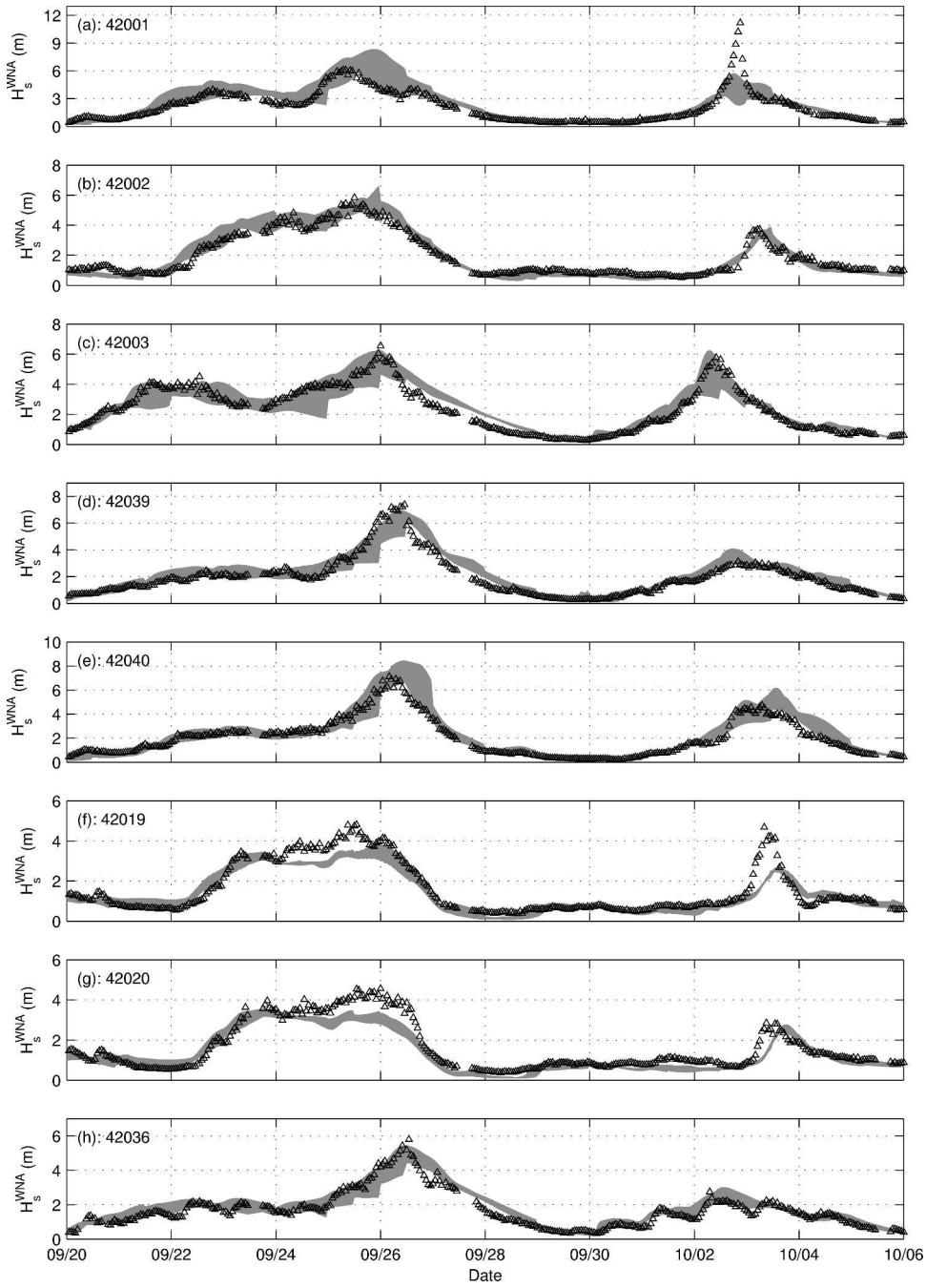

FIG. 8. Forecast envelope for H_s (m) from the WNA model, as in Fig. 6.

lopes from the GFS model, shown in Fig. 10b, retain most of the more relevant properties of the forecast track envelopes of the GFDL model in Fig. 10a. Again, the largest uncertainty in the location of both hurricanes is on the order of 5° of latitude.

Despite the general similarity, Fig. 10 reveals track differences that could potentially affect the wave model forecasts of the WNA and NAH models and explain some of their differences. A comparison between Figs. 10a and 10b indicates that the uncertainty in the GFS forecast tracks for Hurricane Isidore was slightly smaller than that of the GFDL forecasts in both the 24–48- and 48–72-h ranges. The difference was particularly large near buoy 42003, mostly in the 48–72-h range, and in the approach to Isidore's final landfall along the Louisiana coast. The higher inaccuracy of

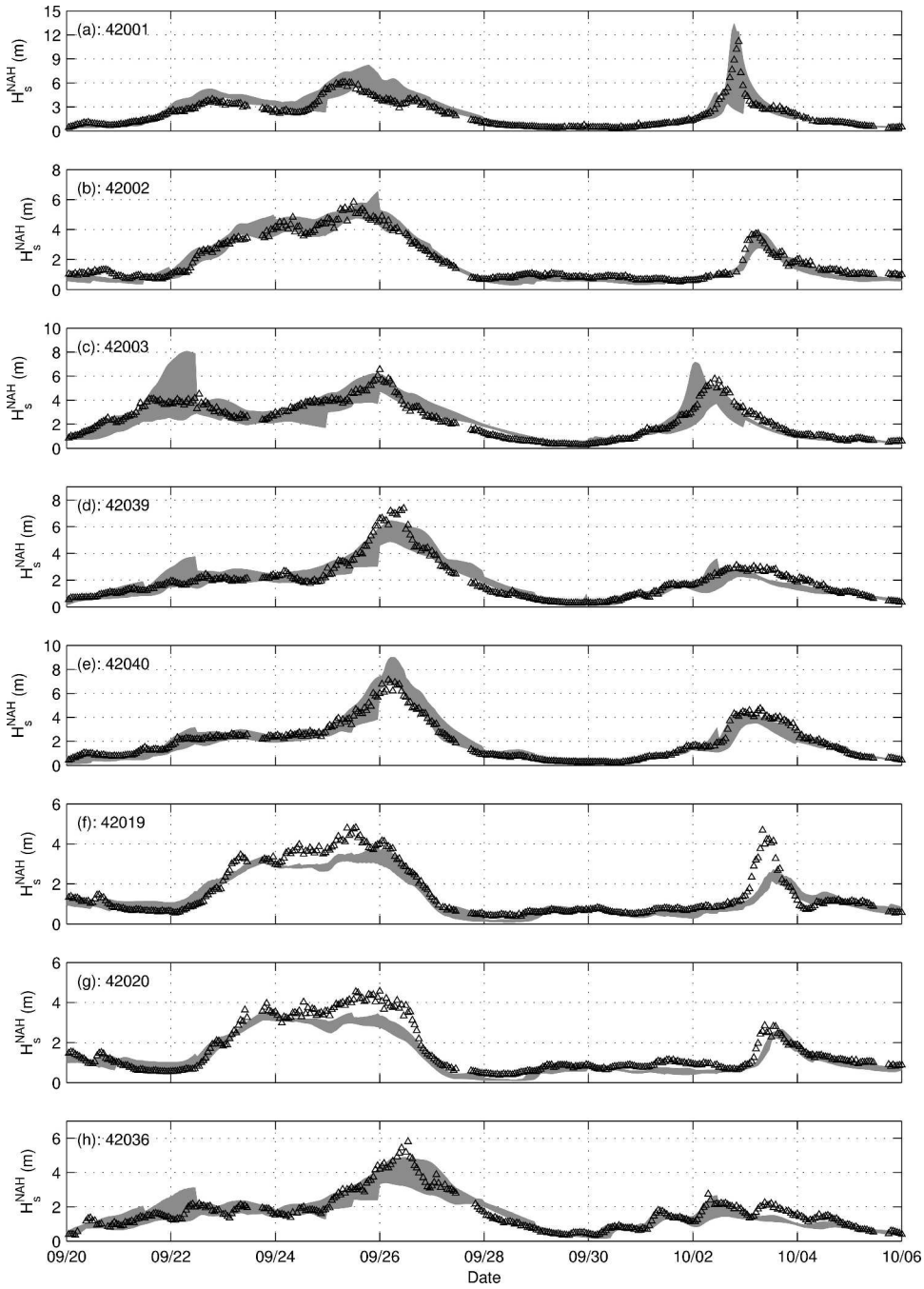

FIG. 9. Forecast envelope for H_s (m) from the NAH model, as in Fig. 6.

GFDL's 48–72-h range forecast in predicting Isidore's approach to buoy 42003 explains the very wide forecast envelope of H_s near 22 September, in the time series for the NAH model, as shown in Figs. 6c and 7c. It may also be related to the wider envelopes in NAH forecast envelopes at buoys 42036 and 42039 on 22 September.

Most of the differences observed in forecast track envelopes during Hurricane Lili for the GFS and GFDL models occurred before the storm entered the Gulf of Mexico, as suggested by Fig. 10. Consequently, the differential effects of track position uncertainties in this case seem to have been overpowered by the more significant differences in the intensity of the surface wind fields in the Gulf, as described in previous sections.

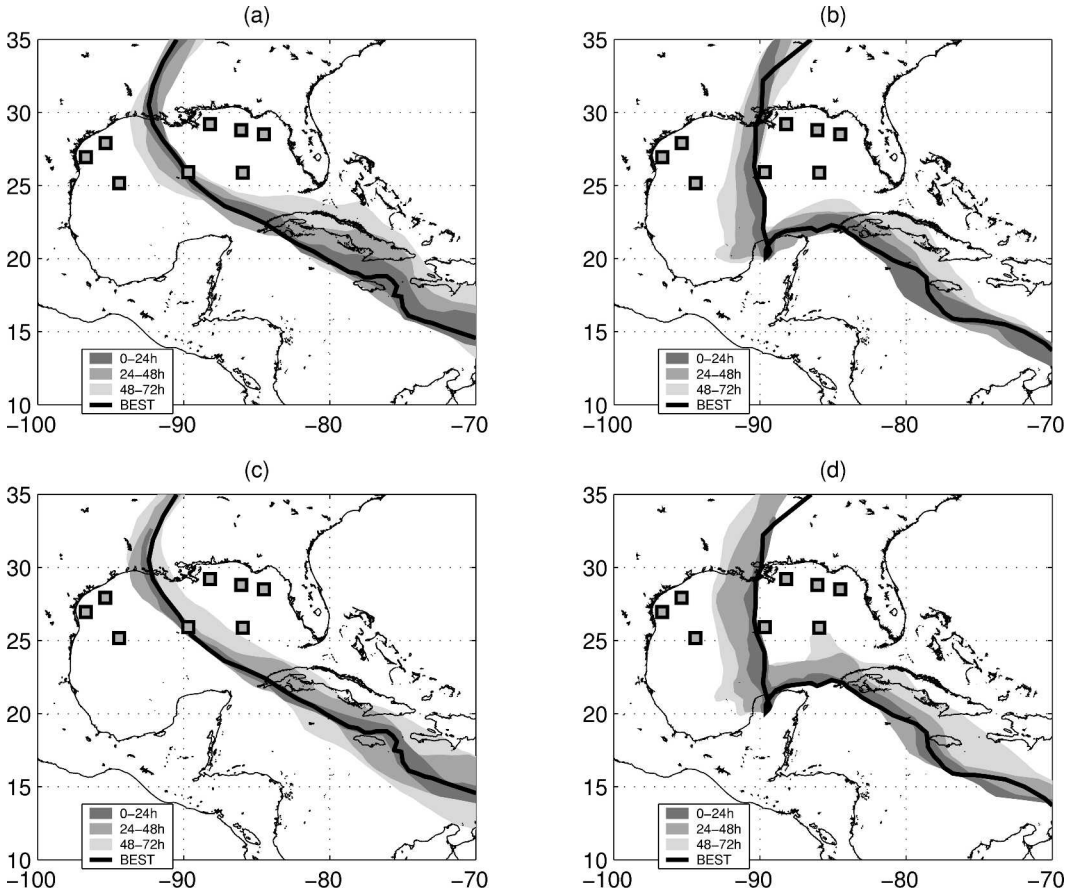

FIG. 10. Model forecast track envelopes for Hurricanes Lili and Isidore at several ranges from 0 to 72 h, shown with the best-track data from NOAA/NHC. Tracks from the (a) WNA and (b) GFS models and the (c) NAH and (d) GFDL model tracks for Hurricanes Lili and Isidore, respectively.

c. Forecasts of extreme storm conditions

A major concern in an operational wave forecasting system is the ability to forecast extreme sea-state conditions during hurricanes. For this reason, in this section we dedicate special attention to investigating the performance of the wave forecasts relative to buoy measurements of the storm maxima. A visual inspection of Fig. 3 suggests that during Hurricane Isidore both the NAH and WNA models had only small differences in forecasts of storm peaks. On the other hand, the differences were significant during Hurricane Lili. Therefore, our analysis of model performance in terms of predicting extreme sea states will focus on wave fields associated with Lili.

To assist in our evaluation of wave model forecasts, we introduce a convenient way of summarizing their ability to predict storm maxima using a "target" diagram, as shown in Fig. 11. The interpretation of this diagram is as follows. We first define acceptable ranges of bias and time lags of model predictions of maximum H_s relative to buoy data, which were chosen presently to be $\pm 20\%$ and ± 3 h. We then define the "target" as a box indicating a region of values satisfying these criteria.

Target plots for the following forecast ranges of maximum waves during Hurricane Lili are shown in Fig. 11: -6 to 0 h, 0 to 12 h, 12 to 24 h, and 36 to 48 h. Target diagrams for the WNA and NAH models are shown in the left- and right-hand-side panels, respectively. Biases are defined as the relative difference between the highest modeled and measured H_s within the envelope of wave heights associated with Lili. Time lags are the time displacements between modeled and observed storm envelopes with higher correlation coefficient.

Figure 11 indicates that forecasts of storm maxima provided by the NAH model were generally within or very near the acceptable ± 3 h range for periods out to the 48-h forecast horizon. WNA model predictions were also on target in terms of time lags, but had a somewhat larger scatter, particularly at larger forecast

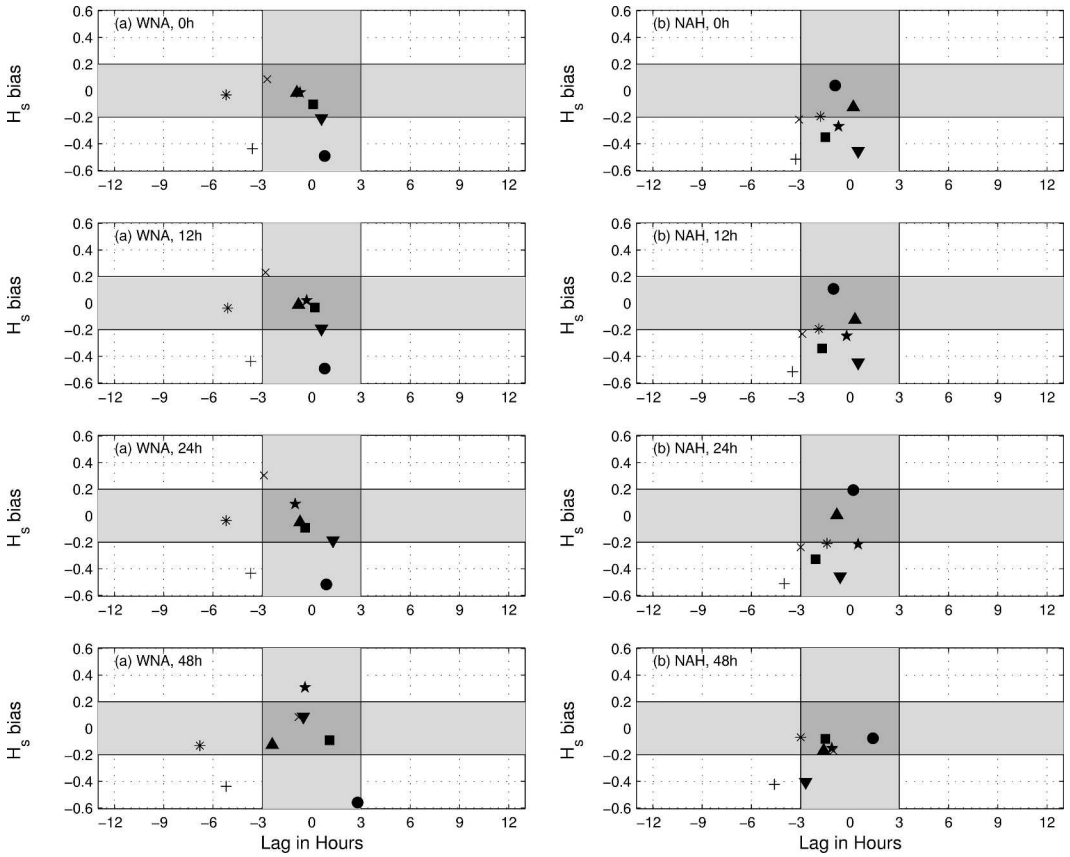

FIG. 11. Accuracy of the NAH model in predicting the maximum waves generated by Hurricane Lili at selected NDBC buoy locations. Buoy patterns: 42001 (filled circle, ●), 42001 (filled triangle, ▲), 42003 (filled square, ■), 42039 (cross, ×), 42040 (star, ★), 42019 (plus sign, +), 42020 (asterisk, *), and 42036 (filled inverted triangle, ▼). See text for approach used for computing maximum H_s bias and time lag.

horizons. WNA data at two buoy locations fell clearly outside the tolerance bounds, whereas all NAH data were within or very near the acceptable bounds. In terms of biases, the cloud of data points from both models seems to indicate that they had similar overall performance. However, a closer look at the data reveals important differences.

Buoy 42001 was the only location directly under Lili's track to provide data representing extreme wave heights generated by Lili. Figure 11 shows that the NAH hindcast of maximum wave height at this location (H_s = 11.6 m) predicted accurately the measured storm maximum wave height (H_s = 11.2 m) in both time of occurrence and intensity. On the other hand, the WNA model hindcast (H_s = 5.7 m) significantly underpredicted the observed wave height at this buoy location.

7. Discussion

The main reason for running specialized hurricane wave models is to use wind forcing generated by an atmospheric model developed specifically for hurricane prediction (e.g., the GFDL model), with high resolution in space and time. This is particularly important because the GFS model used to drive most wave models at NCEP does not have sufficiently high resolution to realistically represent the circulation of small tropical systems. The basic strategy of NCEP's operational hurricane wave models is to use a blended wind field. This consists of a combination of higher-resolution GFDL wind fields around hurricanes with GFS winds in areas not directly under a hurricane's influence.

In this paper, we illustrate the performance of the NAH model for the 2002 Atlantic hurricane season, using results for Hurricanes Isidore and Lili in the Gulf of Mexico. Conventionally, wave model validation is performed for long periods and many observation platforms. Such a comparison between the WNA and NAH models is not relevant, because significant differences occur only for a small number of hurricanes, and mostly for observations relatively close to the track of the hurricanes. Such differences are generally lost in bulk sta-

tistics for longer periods. Hence, case studies are more relevant for model comparison and validation. Case studies, such as the ones presented here, also identify the complexity of the wave conditions generated by an intense hurricane.

It is expected that differences between conventional and hurricane wave models will vary significantly from hurricane to hurricane. Isidore was a very large hurricane, which was well resolved by the GFS. Therefore, GFS and GFDL wind fields were very similar and, consequently, the WNA and NAH models showed virtually identical wave fields. Lili, on the other hand, was small and intense. The GFS model did not resolve and represent Lili's wind fields well, whereas the GFDL model resulted in much more realistic wind conditions. Consequently, extreme waves were much better represented in the NAH model than in the WNA model. It is also clear that the most conspicuous wave model deficiencies, particularly the underestimation of the swell heights from Isidore in the western Gulf in both the WNA and NAH models (Fig. 3; between 24 and 26 September) and during Lili for the NAH model at buoy 42003, appear to be associated with deficiencies in the wind forcing provided by the atmospheric models.

The WNA and NAH models showed nearly identical results for Hurricane Isidore, for which both models suffered equally from using forecast wind fields that did not agree well with the analyzed data. Therefore, the remainder of this discussion will focus on Hurricane Lili, when the different properties of the two wave models seemed more enhanced. Buoy data measured during Lili also provided a wider range of wave evolution scenarios, including extreme waves recorded when the hurricane's maximum wind region moved directly over buoy 42001, in the center of the Gulf of Mexico.

Maximum wave heights observed at buoy 42001 (11.2 m) were well represented by the hindcast of the NAH model (11.6 m), but severely underestimated by the WNA model (5.7 m). The reason for this was the much more realistic description of the core and high wind speed area of Lili by the NAH (GFDL) model, as previously discussed. The top panel in Fig. 9 indicates that the wave forecasts close to the 72-h range were not capturing Lili well. However, this was mostly due to deficiencies in the later forecast ranges. On the other hand, the maximum wave heights at buoy 42001 in the 24- and 48-h forecasts were 12.4 and 12.5 m, respectively. In both cases the occurrence times of the storm maxima were predicted within less than 3 h of the observed maximum wave height time of occurrence. Hence, the NAH model provided accurate guidance for Lili out to the 48-h forecast.

Despite the clear superiority of the NAH model in predicting extreme wave heights at buoy 42001 during Lili, statistics shown in Table 1 indicate that both the WNA and NAH models performed rather poorly at most other buoy locations. The low-resolution GFS winds may explain the poor performance of the WNA model in most situations. One possible explanation for the poor performance of the NAH model, particularly in predicting swell recorded at buoys located away from Lili's path, is the fact that the NAH model hindcast uses GFS analyses blended with short-term *forecasts* from the GFDL model, which does not generate analyzed fields.

Another issue that may be a limiting factor for the accuracy of NAH model forecasts is the wave model itself. It is well known that the existing parameterizations of many wave growth physical processes rely on empirical tuning to be accurate, even in the most advanced numerical wave models. The tuning of the WAVEWATCH III model has been performed using wind forcing provided by the GFS model and its predecessors. Therefore, it may well be that this tuning is not optimal for more accurate hurricane winds.

It is also well known that the present parameterizations of wave physics tend to overestimate the directional width of the spectra. This is expected to have the biggest impact on model results in wind conditions with rapidly changing wind directions, as observed near the core of a hurricane. Furthermore, the parameterizations of wave growth physics used in wave models are based on relatively moderate wind conditions. Recent research (e.g., Powell et al. 2003; Moon et al. 2004) indicates that the extrapolation of these parameterizations to hurricane conditions will lead to an overestimation of surface stresses. This will, therefore, have an impact on wave growth rates, model behavior, and potentially model tuning.

The limitations identified above have been the subject of ongoing wind-wave research activities at NCEP. Also, our results indicate that wave model research may provide a framework for further improvements, particularly from the perceived need for coupling ocean, wave, and wind models for accurate hurricane forecasting in general (e.g., Bender and Ginis 2000; Bao et al. 2000; Moon et al. 2004).

Research at NCEP has also focused on the improvement of parameterizations used in wave models to represent the physics of wave evolution. Some of this research has been explicitly geared to physical processes in hurricane conditions. We believe this framework should provide the means of overcoming some limitations highlighted in the present study.

8. Summary and concluding remarks

This paper describes NCEP's North Atlantic hurricane (NAH) wave model. This model is compared to the conventional western North Atlantic (WNA) model for two severe Atlantic hurricanes in 2002: Isidore and Lili. Both models are validated using buoy data provided by NOAA's National Data Buoy Center (NDBC).

Based on the present investigation and on results reported in previous studies and outlined in section 4, our main conclusions are:

- Blending high-resolution, regional GFDL winds and low-resolution, global GFS surface winds provides a proper framework for predicting hurricane waves.
- The use of case studies provides an effective framework for assessing model performance and incorporates important improvements to hurricane wave forecasting systems.
- Specific properties of hurricane systems, particularly their size, have a strong impact on the quality of surface wind fields generated by the GFS and GFDL models.
- Maximum winds are generally well captured by the GFDL model. However, in large systems such as Isidore the GFS model appeared to provide better winds in the outer sector of the hurricane, with a positive impact on generating swell systems. The poorer outer wind field from the GFDL model was somewhat anomalous for Lili. A recent GFDL model release that has minimized this problem is now used to force NCEP's hurricane-generated wind–wave models, since the 2003 Atlantic hurricane season.
- The use of blended GFS/GFDL winds can produce accurate forecasts of extreme wave heights associated with an intense hurricane out to the 48-h forecast range, despite inaccuracies in the maximum surface wind intensity and location. This may reflect wave growth mechanisms that tend to attenuate small-scale variability in the wind field, but may also result from underestimated maximum GFDL winds being compensated by overestimated surface drag for high winds in the wave model. This important issue is being investigated further as improvements are made to NCEP's wind and wave models.

The performance analysis presented in this study sets the framework for improvements to be incorporated into future implementations of hurricane wave forecasting models at NCEP. These include, potentially, increasing the spatial resolution of wave models in areas under hurricane force winds possibly using multiscale grid systems, coupling wave models with ocean–atmospheric prediction models, and incorporating data assimilation for generating surface wind analyses in operational GFDL model cycles. These issues are currently the subject of ongoing research activities at NCEP.

Acknowledgments. We thank Timothy P. Marchok, Morris Bender, and Robert E. Tuleya, of NOAA's Geophysical Fluid Dynamics Laboratory, for providing valuable information regarding the GFDL hurricane model and providing input data for our hurricane wave model. We also acknowledge the valuable support, observational wave data, and wind analysis products provided by NOAA's National Data Buoy Center (NOAA/NDBC) and Hurricane Research Division (NOAA/HRD).

REFERENCES

Avila, L. A., 2002: Tropical cyclone report: Hurricane Isidore, 14–27, September 2002. NOAA/National Hurricane Center. [Available online at http://www.nhc.noaa.gov/2002isidore.shtml.]

Bao, J.-W., J. M. Wilczak, J.-K. Choi, and L. H. Kantha, 2000: Numerical simulations of air–sea interaction under high wind conditions using a coupled model: A study of hurricane development. *Mon. Wea. Rev.,* **128,** 2190–2210.

Bender, M. A., and I. Ginis, 2000: Real-case simulations of hurricane–ocean interaction using a high-resolution coupled model: Effects on hurricane intensity. *Mon. Wea. Rev.,* **128,** 917–946.

——, ——, T. P. Marchok, and R. E. Tuleya, 2001: Changes to the GFDL hurricane forecast system for 2001 including implementation of the GFDL/URI hurricane–ocean coupled model. Technical Procedures Bulletin 472B, National Weather Service, 15 pp. [Available online at http://www.nws.noaa.gov/om/tpb/.]

——, T. P. Marchok, and R. E. Tuleya, 2002: Changes to the GFDL hurricane forecast system for 2002 including implementation of the 2-nested grid configuration. Technical Procedures Bulletin 492, National Weather Service, 16 pp. [Available online at http://www.nws.noaa.gov/om/tpb/.]

Caplan, P., J. Derber, W. Gemmill, S.-Y. Hong, H.-L. Pan, and D. Parish, 1997: Changes to the NCEP operational medium-range forecast model analysis–forecast system. *Wea. Forecasting,* **12,** 581–594.

Cardone, V. J., R. E. Jensen, D. T. Resion, V. R. Swail, and A. T. Cox, 1996: Evaluation of contemporary ocean wave models in rare extreme events: The Halloween storm of October 1991 and the storm of the century of March 1993. *J. Atmos. Oceanic Technol.,* **13,** 198–230.

Chao, Y., and H. Tolman, 2000: Numerical experiments on predicting hurricane generated wind waves. Preprints, *Sixth Int. Workshop on Wave Hindcasting and Forecasting,* Monterey, CA, U.S. Army Engineer Research and Development Center, 167–179.

——, and ——, 2001: Specification of hurricane wind fields for ocean wave prediction. *Proc. Fourth Int. Symp. on Waves: Ocean Wave Measurement and Analysis,* Vol. 1, San Francisco, CA, Office of Naval Research, 671–679.

——, L. Burroughs, and H. Tolman, 1999a: Wave forecasting for Alaskan waters. Technical Procedures Bulletin 496, National Weather Service. [Available online at http://polar.ncep.noaa.gov/omb/tpbs/tpb496.]

——, ——, and ——, 1999b: Wave forecasting for the western North Atlantic and adjacent waters. Technical Procedures Bulletin 495, National Weather Service. [Available online at http://polar.ncep.noaa.gov/omb/tpbs/tpb495.]

——, ——, and ——, 2001: The North Atlantic hurricane wind wave forecasting system. Technical Procedures Bulletin 478, National Weather Service. [Available online at http://polar.ncep.noaa.gov/omb/tpbs.]

——, ——, and ——, 2002: Wave forecasting for the eastern North Pacific and adjacent waters. Technical Procedures Bulletin 491, National Weather Service. [Available online at http://polar.ncep.noaa.gov/omb/tpbs/tpb491.]

Kurihara, Y., R. E. Tuleya, and M. A. Bender, 1998: The GFDL hurricane prediction system and its performance in the 1995 hurricane season. *Mon. Wea. Rev.,* **126,** 1306–1322.

Lawrence, M. B., 2002: Tropical cyclone report: Hurricane Lili, 21 September–04 October 2002. National Hurricane Center. [Available online at http://www.nhc.noaa.gov/2002lili.shtml.]

Liu, Q., T. Marchok, H.-L. Pan, B. Morris, and S. Lord, 2000: Improvements in hurricane initialization and forecasting at NCEP with global and regional GFDL models. Technical Procedures Bulletin 472, National Weather Service, 7 pp. [Available online at http://www.nws.noaa.gov/om/tpb/.]

Moon, I. J., T. Hara, I. Ginnis, S. E. Belcher, and H. L. Tolman, 2004: Effect of surface waves on air–sea momentum exchange. Part I: Effect of mature and growing seas. *J. Atmos. Sci.,* **61,** 2321–2333.

Moorthi, S., H.-L. Pan, and P. Caplan, 2001: Changes to the 2001 NCEP operational MRF/AVN global analysis/forecast system. Technical Procedures Bulletin 484, National Weather Service, 14 pp. [Available online at http://www.nws.noaa.gov/om/tpb/.]

Powell, M. D., S. H. Houston, L. R. Amat, and N. Morisseau-Leroy, 1998: The HRD real-time hurricane wind analysis system. *J. Wind Eng. Indust. Aerodyn.,* **77/78,** 53–64.

——, ——, ——, and T. A. Reinhold, 2003: Reduced drag coefficient for high wind speeds in tropical cyclones. *Nature,* **442,** 279–283.

Surgi, N., H.-L. Pan, and S. J. Lord, 1998: Improvement of the NCEP global model over the Tropics: An evaluation of model performance during the 1995 hurricane season. *Mon. Wea. Rev.,* **126,** 1287–1305.

Tolman, H. L., 1998: Validation of NCEP's ocean winds for the use in wind wave models. *Global Oceanic Atmos. Syst.,* **6,** 243–268.

——, B. Balasubramaniyan, L. D. Burroughs, D. V. Chalikov, Y. Y. Chao, H. S. Chen, and V. V. Gerald, 2002: Development and implementation of wind-generated ocean surface wave models. *Wea. Forecasting,* **17,** 311–333.

——, J. H. G. M. Alves, and Y. Y. Chao, 2005: Operational forecasting of wind-generated waves by Hurricane Isabel at NCEP. *Wea. Forecasting,* **20,** 544–557.